Application of Nanotechnology in Removal of NAPLs from Contaminated Aquifers – A Source Clean-up Experimental Study

Tannaz Pak[1*], Nathaly Lopes Archilha[2], Raaid Al-Imari[1]

[1]Teesside University, [2] Brazilian Synchrotron Light Laboratory (LNLS)

Email: t.pak@tees.ac.uk, T: +44 (0)1642 342466

ORCID: Tannaz Pak (0000-0001-7635-9333), Nathaly Lopes Archilha (0000-0003-0324-3748)

Keywords: Nanotechnology, Porous media, Removal of organic contaminants, Nonaqueous phase liquids (NAPLs)

Abstract

This work investigates the removal of non-aqueous phase liquids (NAPLs) from groundwater resources using nanotechnology. We present results of a series of multiphase fluid displacement experiments conducted in a naturally occurring sandstone rock. These experiments involve injection of an aqueous suspension of silica nanoparticles to remove a trapped NAPL phase. Specifically, the effect of nanoparticle concentration on the efficiency of the NAPL removal is studied. Our results show that silica nanoparticles successfully remobilised the trapped NAPL phase and resulted in 13% increase in its removal efficiency. The optimal concentration for NAPL removal efficiency is found to be 0.3 wt%.

1. Introduction

Cleaning the subsurface groundwater resources contaminated with nonaqueous phase liquids (NAPLs) have been the subject of extensive research in the recent decades (Soga, Pagea and Illangasekare, 2004; Trellu *et al.*, 2016). New technologies which offer effective contaminant removal efficiencies at lower costs are always in demand. When dealing with removal of NALP form contamination source (i.e. source remediation) the main mechanism to overcome is capillary trapping (Wilson, 1990). It is well-established that removal of a non-wetting fluid from porous media by injection of the wetting phase is always less than 100% efficient (Wilson, 1990). The wetting phase is a fluid that has a higher tendency to spread on a solid surface in presence of another non-wetting fluid (Craig, 1971). As a result, a portion of a non-wetting phase will remain trapped in the porous media. Capillary trapping has previously been directly observed in micro-model studies (Jeong, Corapcioglu and Roosevelt, 2000). More recently, non-destructive 3D imaging techniques, such as X-ray computed micro-tomography, have enabled direct observation of capillary trapping of non-wetting fluids in naturally occurring porous media (Iglauer *et al.*, 2011; Berg *et al.*, 2013; Pak *et al.*, 2015). Capillary trapping is governed by the competition between the capillary, viscous, and gravitational forces. Specifically, the relative importance of the viscous to capillary

forces is measured using capillary number (Nc=μV/σ) where μ is viscosity (Pa.s), V isvelocity (m/s) and σ is the interfacial tension (IFT) in N/m.

Bioremediation is one of the widely practiced and cost-effective technologies that uses microbes to degrade the contaminant in-situ (Aulenta, Majone and Tandoi, 2006; Daghio *et al.*, 2017). Another successful NAPL removal method involves injection of surfactants to reduce the IFT between the aqueous and the oil phases (Mulligan, Yong and Gibbs, 2001; Paria, 2008; Cheraghian and Hendraningrat, 2016). This reduces the capillary forces and hence eases the remobilisation and removal of the trapped NAPL phase. Within this context, among the more recent technologies is the use of nanofluids (nanoparticle suspensions) to improve the efficiency of NAPL removal at microscopic level. More specifically, reactive nanoparticles (NPs) such as zero-valent iron (Fe^0) NPs are successful in in-situ degradation of some contaminants (specifically chlorinated ones) into less harmful ones (Tosco *et al.*, 2014). Further, recent developments in industrial scale manufacturing of engineered NPs at low cost makes NP-based NAPL removal an attractive option. However, although promising, the health implications of long-term exposure to reactive particles such as Fe^0 are not yet fully understood, i.e. the environmental aspects of this technology requires further research (Bardos *et al.*, 2011). In this sense, NPs with better biocompatibility are more favourable. Specifically, silica NPs have been safely used in diagnosis and target drug delivery in the bio-medical field, widely (Santra *et al.*, 2004; Jin *et al.*, 2007; Bharti *et al.*, 2015). Silica-based NAPL removal method is hence a more environmentally friendly candidate. Literature studies have shown that silica, alumina, and titanium oxide nanoparticles are suitable candidates for designing nanotechnology-based enhanced oil recovery processes (Ogolo, Olafuyi and Onyekonwu, 2012; Ahmadi *et al.*, 2013; Hendraningrat, Li and Torsæter, 2013; Roustaei, Saffarzadeh and Mohammadi, 2013; Bennetzen and Mogensen, 2014; Zhang *et al.*, 2014; Hendraningrat and Torsæter, 2015; Negin, Ali and Xie, 2016).

This work investigates the effect of nanofluid concentration on the recovery efficiency of NAPLs from a naturally occurring sandstone. In our experiments, we

used hydrophilic 30-nm silica NPs, in three different concentrations of 0.1, 0.3 and 0.5 wt%. We monitored the fluid pressure drop as well as the concentrations of NPs in the effluent. This allowed determining the NP retention in the rock. In addition to the removal of NAPL contaminants form water resources. Results of this study has implications for a broad range of applications, including enhanced hydrocarbon recovery from geological formations and secure CO_2 storage in the carbon capture and storage (CCS) process.

2. Materials and Methods

Materials: At nanoscale matters display high surface area per unit volume when compared to larger scales. Therefore, nanomaterial are known to show properties closer to the behaviour of individual molecules (Khler and Fritzsche, 2004). For instance, a substance may not dissolve in water at macro scale while it may be easily soluble in water at nanoscale. Nanofluids are referred to fluids that consist of a base fluid (aqueous or organic) with nano-sized particles (< 100 nm) dispersed in them. A key property of nanofluids that rules the effectiveness of their application is their stability which needs to be closely monitored when designing a NP-based NAPL removal process (Metin *et al.*, 2011; Yu and Xie, 2012).

We performed fluid displacement experiments in a cylindrical core plug (D=2.53 cm, L=6.23 cm) from a water-wet Scottish sandstone outcrop (Locharbriggs). Laboratory measurements showed effective porosity of 23.3% and the permeability of 284.9 mD for this core sample. Scanning electron microscopy images (See Figure S1 in the supporting information) show the pore-sizes in this sandstone are in the range of tens of μm. Analysis of oil/water displacement experiments (see Figure S2 in the supporting information) show that the pore-throat sizes are in the range of a few μm. This makes the pore structure of this sandstone sufficiently open to allow transport of stable suspensions of nanoparticles. It should be noted that the pore-throat size distribution of a porous material is accurately determined using the mercury intrusion porosimetry

technique. Nevertheless, an approximate estimate of the size range of pore-throats could be obtained by employing the pressure drop signal of oil/water drainage step. The nanofluids were prepared by diluting a highly concentrated (25%) suspension of hydrophilic silica NPs (APS = 30 nm) to achieve 0.1, 0.3, and 0.5 wt%. We used both deionized water and brine (3 wt% NaCl) for this dilution. To maximize colloidal suspension the diluted nanofluids were placed in an ultrasonic bath for 30 minutes. Viscosity of the nanofluids shows changes insignificant to the flow processes studied here, i.e. only ~1%, hence viscosity is assumed to be equal to that of water. A mineral oil (n-decane) was used as the NAPL phase.

Experimental Set-up and Fluid Displacement Test Procedure: Figure 1 shows a schematic of the experimental setup used in this study. The tests comprised of fluid injections (oil/water/nanofluid) while monitoring the effluent fluid as well as recording the pressure drop across the core plug. The outlet stream was open to atmospheric pressure and the experiment was conducted under ambient temperature. Initially, the core plug was vacuum saturated with the aqueous solution. After loading the core in this set-up the confining pressure of 1000 psi was applied to ensure the fluid flow is one-dimensional, i.e. from the core inlet to its outlet. During the flow process the differential pressure (ΔP) across the core was recorded every 30 seconds. Subsequently, the oil was injected at three different flowrates (1 mL/min, 3 mL/min and 4 mL/min) until no more brine was produced. This was to ensure the core contains a substantial amount of oil before the subsequent displacements were performed. At this point, 22 pore volumes of oil were injected in the core.

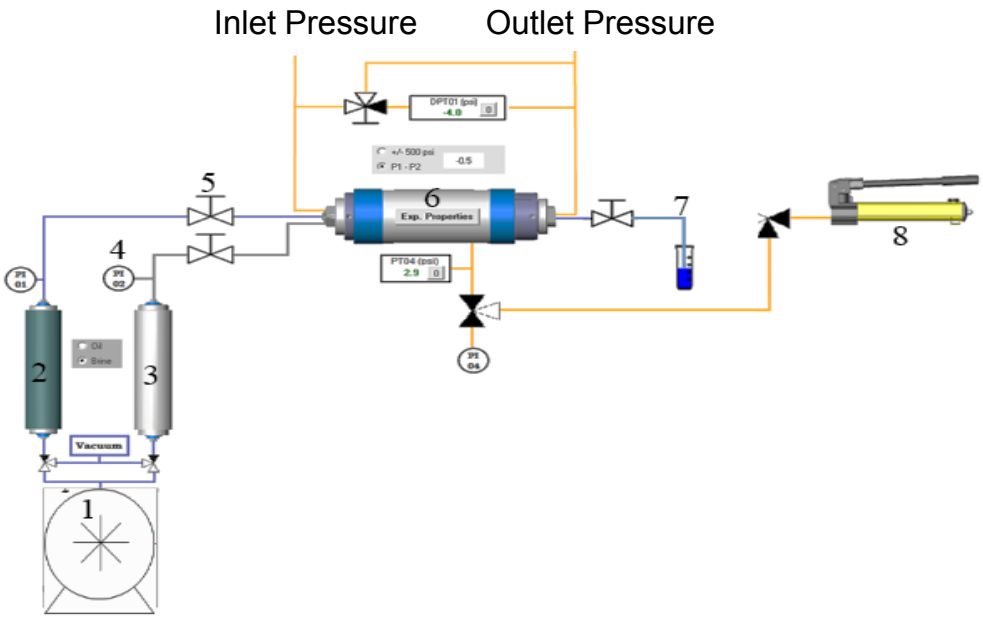

Figure 1: *Experimental setup, (1)* pump, *(*2) oil reservoir, *(*3) water reservoir, *(*4) pressure gauges, *(*5) valves, *(*6) flow cell (Hassler type), *(*7) effluent into test tubes, *(*8) *c*onfining pressure pump.

After the initial oil saturation, the fluids were injected at a constant rate of 0.25 mL/min, equivalent to 3.4% pore-volume/min. This is equivalent to capillary numbers (Nc) in the order of 10^{-7}, which ensures that the fluid displacements are representative of flow at aquifer scale. The next stage was water injection until no more oil was produced, which established the residual oil saturation (S_{or}). The experiment continued by injecting nanofluids at three different concentrations of 0.1, 0.3, and 0.5 wt%. Any additional oil produced at these stages indicates the effectiveness of nanofluid injections in remobilisation of the trapped oil. At all injection steps, samples of the effluent fluids were collected at the core outlet. This allowed measuring the amount of oil and nanofluid remained in the core using the principle of material balance. These values were used for calculation of fluid saturations and the NAPL removal efficiency. The NP retention curve was also plotted by analysing these samples.

Analysis of the Effluent Samples and IFT Measurement: The ultraviolet–visible (UV) spectrometry was used to measure the concentration of NPs in the effluent

fluid. Figure 2 shows the UV absorbance response for deionised water and the nanofluids at the three concentrations used in this study. This is a calibration curve that was used to find the concentration of NPs in the effluent samples based on their UV absorbance.

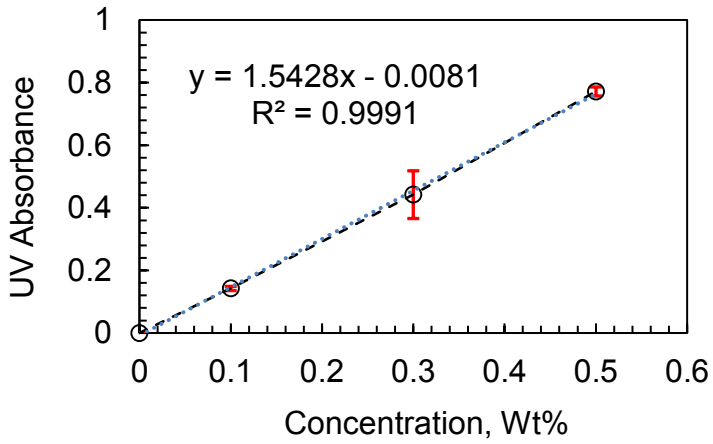

Figure 2: Calibration curve used to find nanofluid concentration based on its UV absorbance.

IFT was measured using the Du Nouy ring method (Macy, 1935), which works with raising a ring initially immersed in a liquid into a second liquid sitting on the top.

3. Results and Discussion

Nanofluid Stability: The brine-based nanofluids (3 wt%, NaCl) showed significant instability which resulted in agglomerations of NPs. Figure 3 shows the brine-based nanofluids at various concentrations on the day of preparation (A) and after two days (B). The nanofluid became cloudy resulting in NP aggregation and sedimentation.

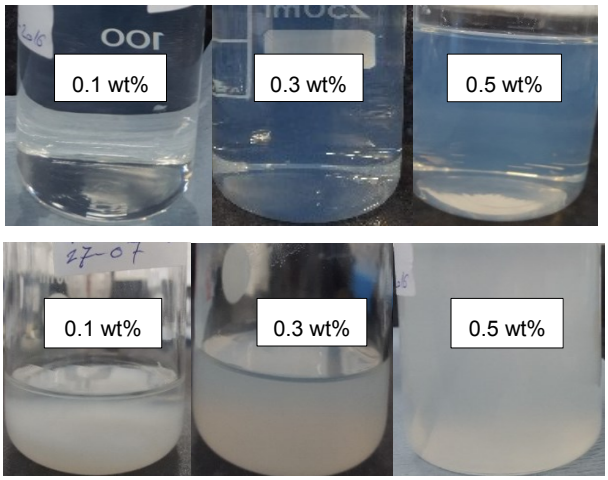

Figure 3: Brine-based (3 wt%, NaCl) nanofluids at three concentrations of 0.1, 0.3, and 0.5 wt%), (A) on the day of preparation, and (B) after two days.

The salinity of these brine-based nanofluids, i.e. 3 wt%, is higher than the NaCl's critical salt concentration (CSC). CSC is the maximum salt concentration at which the stability can be achieved. To achieve better stability, one should use smaller NPs or reduce the salt concentrations. Here, the 3 wt% concentration was used to represent aquifers with average salinity. Temperature is another parameter that affects colloidal stability. At higher temperatures the CSC decreases making the application of brine-based nanofluids more challenging for injection in geological formations with high temperatures. Water-based nanofluids were stable.

Interfacial Tension: For the water-based nanofluids, the IFT decreases as the nanofluids concentration increases (Figure 4). The 0.3 wt% water-based nanofluid showed the minimum IFT, i.e. 29.6 mN/m, this represents a reduction of 18% compared to the oil/water system. At of 0.5 wt% concentration the nanofluid instability causes the IFT to measure at 35.06mN/m, a value very close to the original oil/water system (36.06 mN/m).

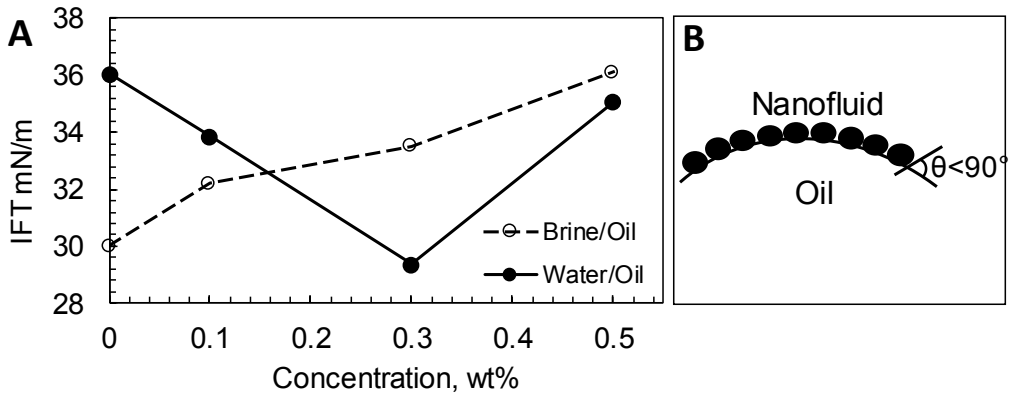

Figure 4: (A) IFT as a function of nanofluid concentration, (B) NPs position themselves at the oil/water interface, acting as surfactant molecules (Binks, 2002)

The reduction in IFT is due to adsorption of NPs to the fluid/fluid interface (Figure 4B). Silica is hydrophilic, therefore, the bulk of the particles preferably remains within the aqueous phase. The fluid/solid contact surfaces have lower energy levels compared to fluid/fluid interfaces. As a result, the system will have a lower total interfacial energy with the particles adsorbed the fluid/fluid interface (Binks, 2002).

The brine-based nanofluids showed an increasing trend with the NP concentration. This also confirms the brine-based nanofluids were unstable suspensions. Therefore, for the subsequent fluid displacement experiments we only used the water-based nanofluids.

NAPL Removal Efficiency: Figure 5 shows the remaining NAPL saturation after the four oil displacement steps (i.e. water and nanofluid injections). Initially, 72.6% of the pore space was occupied with the NAPL phase, making the water saturation 27.4%. The water injection resulted in production of 64% of this NAPL phase, reducing the remaining NAPL saturation to 26.13%.

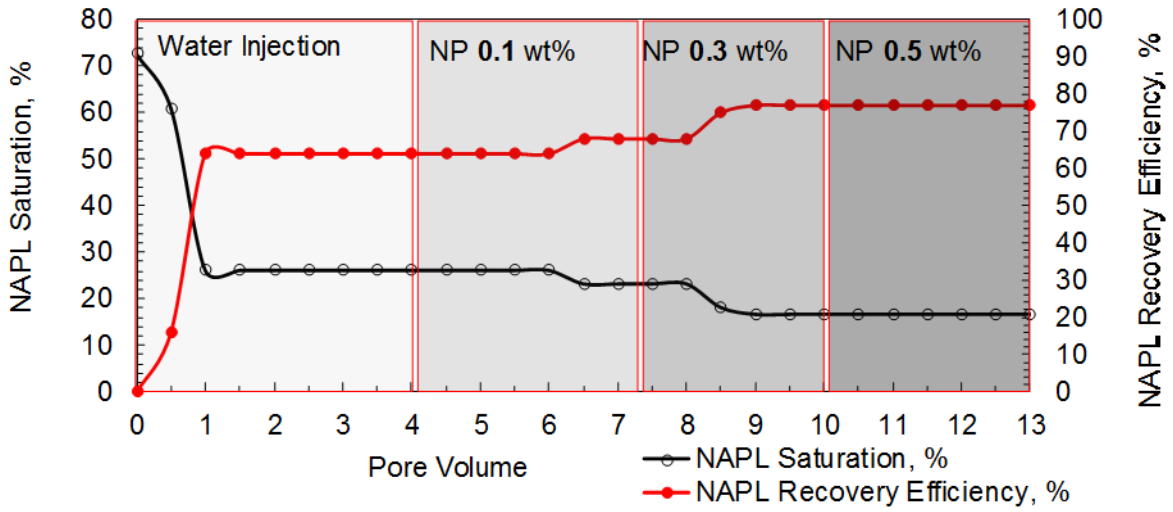

Figure 5: NAPL saturation during the fluid displacement steps.

As shown the NAPL production has occurred during the first PV of water injection. This behaviour is an indication of a water-wet system where the non-wetting fluid becomes trapped in a single pore or within multiple connecting pores, surrounded by the wetting corner films (Berg *et al.*, 2013; Pak, 2015). It is, therefore, impossible to produce this remaining oil unless one or more of the key parameters controlling the capillary trapping are changed. These include the flow regime, rock wettability, and fluid/fluid IFT. Here, the introduction of the nanofluids targets the IFT alteration. It should be noted that in cases where the rock is preferentially oil wet the effect of nanofluids can be two-folds impacting both the wettability and IFT (Li and Torsæter, 2015).

The subsequent injections of the nanofluids further reduced the NAPL saturation to 23.23% and 16.69%, respectively for the 0.1 and 0.3 wt% concentrations. This corresponds to increase of the recovery efficiency to 68% and 78%, respectively. No more additional oil was produced by injecting nanofluid at 0.5 wt% concentration. This can be explained by the IFT vs NP concentration trend, shown in Figure 4A. At 0.5 wt% the water-based nanoparticle solution becomes unstable showing an IFT close to that of the water/oil IFT with no NPs in. Therefore, our results suggest that unstable suspensions have little effect on IFT and hence NAPL removal.

Nanoparticle Retention: The studied particle-rock pair was selected such that the particle attraction to the rock surface and hence the particle retention in the core is minimised. The particle adsorption onto the rock surface is controlled by the balance of the attractive/repulsive forces between the particles and the rock surface. Zeta potential measurement reflects this resultant force (Hunter, 1981). This sandstone is mainly composed of quartz (i.e. SiO_2) mineral. Zeta potential analysis on powdered samples of this rock measured values of -19.5 mV at pH~7. From the literature the zeta potential for silica nanoparticles is measured to be close to -30 mV at pH~7 (Kumar *et al.*, 2004). Therefore, no particle-particle and particle-rock attraction is expected. Hence, particle retention on this sandstone should be negligible.

An insignificant increase in the differential pressure across the core plug was observed during the nanofluid injection steps compared to water injection step. As shown in Figure 6, the pressure drop increases with increase in particle concentrations. The injection flow rate was kept constant, hence the increased differential pressure reflects some progressive pore-structure clogging caused by particle entrapment within the rock. It is well-established that when transported in porous media, nanofluids lose a portion of their particles through adsorption to the solid surface (Bradford and Torkzaban, 2008). The amount and pattern of this retention has implications for transport properties of the porous media (e.g. permeability), therefore, measuring NP retention is critical in designing a successful nanofluid-based NAPL removal process. Here the permeability is measured to decrease from 284.904 mD to 227.92 mD, 183.15 mD, and 170.94 mD for the nanofluid injection steps at 0.1 wt%, 0.3 wt% and 0.5 wt% concentrations, respectively. It should be noted that these measurements are end point relative permeability values calculated based on the pressure drop recorded at the end of each fluid injection step (Figure 6). These measurements suggest that although the relative permeability has decreased, it has remained within the same order of magnitude as the absolute permeability, making nanofluid injection a feasible option for NAPL removal from this rock.

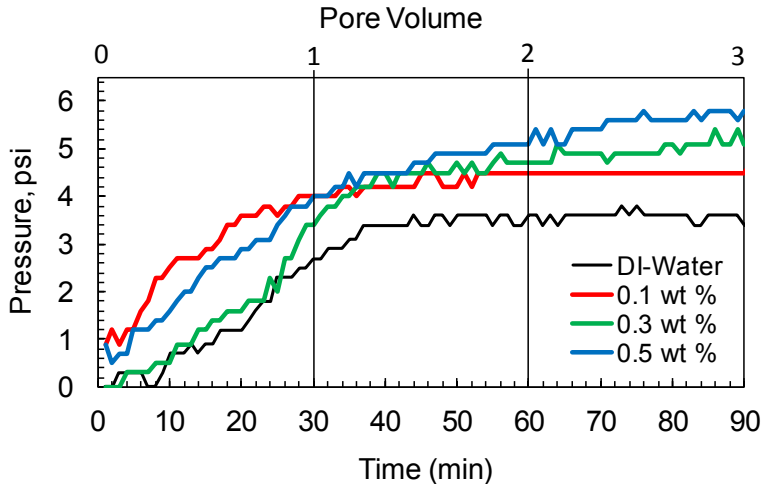

Figure 6: Pressure drop across the core, recorded during the injection steps.

Figure 2 shows the optical absorbance of nanofluids at 228 nm wavelength. For nanoparticle concertation of 0.1 wt%, 0.3 wt% and 0.5 wt% there is a linear relationship between the concentration and the optical absorbance. This calibration curve was used to determine the nanoparticle concentration of effluent fluids. The adsorption-desorption of NPs on the pore walls should eventually reach an equilibrium with continuous injection. As a result, the NP concentration of the effluent fluid will increase over time. For our experiment, the maximum adsorption capacity of the rock is reached after the 1.5 PVs of fluid injection (Figure 7). Beyond this point, the pressure drop and the effluent's NP concentrations have converged to constant values. This convergence point depends on the NP/rock interaction, available rock surface area, and the heterogeneity of the pore-structure.

Figure 7 shows the retention (breakthrough) curves (Ben-Moshe, Dror and Berkowitz, 2010; Wang *et al.*, 2012) for the injections performed in this study. Both effluent NP concentration and dimensionless concentrations (i.e. the ratio of NPs concentration in the effluent to that of the injected fluid) are shown on this plot. After injection of 1.5 PVs 91% to 97 % of the injected NPs reach the core outlet. Due to the stability of the nanofluids as well as the significant difference between the NPs size and that of rock pore-throats (order of micro-meters) for this highly permeable sandstone shows no significant pore-space clogging.

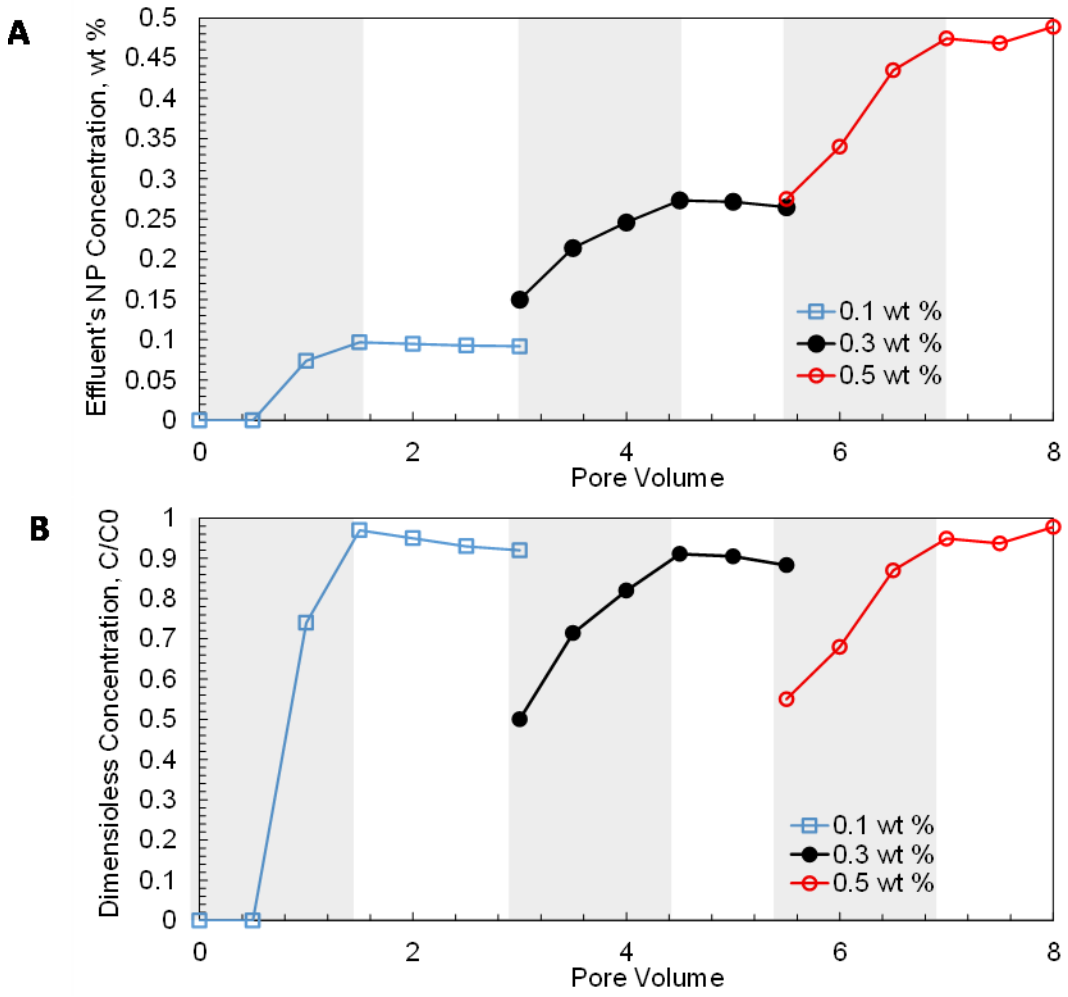

Figure 7: Nanoparticles breakthrough curves, (A) Nanoparticle concentration, (B) Dimensionless concentration normalised by the injection concentration

Pore

4. Conclusions

This paper presents the results of a series of multiphase fluid flow injections in porous media to investigate the effectiveness of silica-nanofluids in removal of NAPL fluids from contaminated porous media. Specifically, this study investigates remediation of contamination sources using immiscible displacement processes. Our experiments show that:

1. Silica-nanofluid has successfully remobilised the trapped contaminant phase, reducing its saturation by 9.44%. This is equivalent to 13% improvement in the recovery efficiency.
2. For the fluid pair and the NPs under study the optimum NP concentration in terms of NAPL removal is 0.3 wt%.
3. The main mechanism which increased the NAPL recovery is the reduction in IFT, with NPs acting as surfactants.
4. To achieve an effective NAPL removal the primary requirement is to have a stable nanofluid suspension and controlled particle retention.

The presented analysis show that only a small fraction of NPs was retained in the sandstone core due to the negative surface charge of the particles and the rock. This particle retention caused only minor increase in the required injection pressure during the nanofluid injection steps. This is mainly due to the rock's high permeability and the significant difference between the NP size (controlled by suspension stability) and the pore-throat sizes. As a result, the studied NPs/fluids/rock combination are suitable for NP-based remediation.

Acknowledgements:

This project was partly supported by the Royal Academy of Engineering under the Newton Research Collaboration Programme (Academy Reference: NRCP1516/1/159). We thank Jeffrey Lawrence, Marwan Rezk, and Richard Medd for their helps in SEM imaging and Zeta potential measurements.

References:

Ahmadi, M. *et al.* (2013) 'Zeta-potential investigation and experimental study of nanoparticles deposited on rock surface to reduce fines migration', *SPE Journal*, 18(3), pp. 534–544. doi: 10.2118/142633-PA.

Aulenta, F., Majone, M. and Tandoi, V. (2006) 'Enhanced anaerobic bioremediation of chlorinated solvents: environmental factors influencing microbial activity and their relevance under field conditions', *Journal of Chemical Technology*

301 *& Biotechnology*. John Wiley & Sons, Ltd., 81(9), pp. 1463–1474. doi:
302 10.1002/jctb.1567.
303 Bardos, R. *et al.* (2011) 'A risk/benefit approach to the application of iron
304 nanoparticles for the remediation of contaminated sites in the environment'.
305 Available at: http://eprints.brighton.ac.uk/14887/1/CB0440FInalReport.pdf
306 (Accessed: 31 July 2017).
307 Ben-Moshe, T., Dror, I. and Berkowitz, B. (2010) 'Transport of metal oxide
308 nanoparticles in saturated porous media', *Chemosphere*, 81(3), pp. 387–393. doi:
309 10.1016/j.chemosphere.2010.07.007.
310 Bennetzen, M. V. and Mogensen, K. (2014) 'Novel Applications of Nanoparticles
311 for Future Enhanced Oil Recovery', *International Petroleum Technology*
312 *Conference*, (December), pp. 10–12. doi: 10.2523/17857-MS.
313 Berg, S. *et al.* (2013) 'Real-time 3D imaging of Haines jumps in porous media
314 flow.', *Proceedings of the National Academy of Sciences of the United States of*
315 *America*. National Academy of Sciences, 110(10), pp. 3755–9. doi:
316 10.1073/pnas.1221373110.
317 Bharti, C. *et al.* (2015) 'Mesoporous silica nanoparticles in target drug delivery
318 system: A review.', *International journal of pharmaceutical investigation*. Medknow
319 Publications, 5(3), pp. 124–33. doi: 10.4103/2230-973X.160844.
320 Binks, B. (2002) 'Particles as surfactants—similarities and differences', *Current*
321 *Opinion in Colloid & Interface Science*, 7(1), pp. 21–41. doi: 10.1016/S1359-
322 0294(02)00008-0.
323 Bradford, S. A. and Torkzaban, S. (2008) 'Colloid Transport and Retention in
324 Unsaturated Porous Media: A Review of Interface-, Collector-, and Pore-Scale
325 Processes and Models', *Vadose Zone Journal*. Soil Science Society, 7(2), p. 667.
326 doi: 10.2136/vzj2007.0092.
327 Cheraghian, G. and Hendraningrat, L. (2016) 'A review on applications of
328 nanotechnology in the enhanced oil recovery part A: effects of nanoparticles on
329 interfacial tension', *International Nano Letters*, 6(2), pp. 129–138. doi:
330 10.1007/s40089-015-0173-4.
331 Craig, F. F. (1971) *The reservoir engineering aspects of waterflooding*. H.L.

Doherty Memorial Fund of AIME. Available at: http://store.spe.org/The-Reservoir-Engineering-Aspects-Of-Waterflooding--P68.aspx (Accessed: 21 May 2017).

Daghio, M. *et al.* (2017) 'Electrobioremediation of oil spills', *Water Research*, 114, pp. 351–370. doi: 10.1016/j.watres.2017.02.030.

Hendraningrat, L., Li, S. and Torsæter, O. (2013) 'A coreflood investigation of nanofluid enhanced oil recovery', *Journal of Petroleum Science and Engineering*, 111, pp. 128–138. doi: 10.1016/j.petrol.2013.07.003.

Hendraningrat, L. and Torsæter, O. (2015) 'A Stabilizer that Enhances the Oil Recovery Process Using Silica-Based Nanofluids', *Transport in Porous Media*. Springer Netherlands, 108(3), pp. 679–696. doi: 10.1007/s11242-015-0495-8.

Hunter, R. J. (1981) *Zeta Potential in Colloid Science: Principles and Applications*, *Trends in Food Science & Technology*. doi: 10.1016/S0924-2244(97)01001-7.

Iglauer, S. *et al.* (2011) 'Residual CO_2 imaged with X-ray micro-tomography', *Geophysical Research Letters*, 38(21), p. n/a-n/a. doi: 10.1029/2011GL049680.

Jeong, S.-W., Corapcioglu, M. Y. and Roosevelt, S. E. (2000) 'Micromodel Study of Surfactant Foam Remediation of Residual Trichloroethylene'. American Chemical Society. doi: 10.1021/ES9910558.

Jin, Y. *et al.* (2007) 'Toxicity of luminescent silica nanoparticles to living cells', *Chemical Research in Toxicology*, 20(8), pp. 1126–1133. doi: 10.1021/tx7001959.

Khler, M. and Fritzsche, W. (2004) *Nanotechnology : an Introduction to Nanostructuring Techniques.* Wiley-VCH.

Kumar, M. N. R. *et al.* (2004) 'Cationic silica nanoparticles as gene carriers: synthesis, characterization and transfection efficiency in vitro and in vivo.', *J Nanosci Nanotechnol*, 4(7), pp. 876–881. doi: 10.1166/jnn.2004.120.

Li, S. and Torsæter, O. (2015) 'The Impact of Nanoparticles Adsorption and Transport on Wettability Alteration of Intermediate Wet Berea Sandstone', in *SPE-172943-MS* . SPE. Available at: https://www.onepetro.org/download/conference-paper/SPE-172943-MS?id=conference-paper%2FSPE-172943-MS (Accessed: 4 May 2017).

Macy, R. (1935) 'Surface tension by the ring method. Applicability of the du Nouy apparatus', *Journal of Chemical Education*. Division of Chemical Education ,

12(12), p. 573. doi: 10.1021/ed012p573.
Metin, C. O. *et al.* (2011) 'Stability of aqueous silica nanoparticle dispersions', *Journal of Nanoparticle Research*, 13(2), pp. 839–850. doi: 10.1007/s11051-010-0085-1.
Mulligan, C. ., Yong, R. . and Gibbs, B. . (2001) 'Surfactant-enhanced remediation of contaminated soil: a review', *Engineering Geology*, 60(1), pp. 371–380. doi: 10.1016/S0013-7952(00)00117-4.
Negin, C., Ali, S. and Xie, Q. (2016) 'Application of nanotechnology for enhancing oil recovery – A review', *Petroleum*, 2(4), pp. 324–333. doi: 10.1016/j.petlm.2016.10.002.
Ogolo, N., Olafuyi, O. and Onyekonwu, M. (2012) 'Enhanced Oil Recovery Using Nanoparticles', *Saudi Arabia Section Technical Symposium and Exhibition*, p. 9. doi: 10.2118/160847-MS.
Pak, T. *et al.* (2015) 'Droplet fragmentation: 3D imaging of a previously unidentified pore-scale process during multiphase flow in porous media', *Proceedings of the National Academy of Sciences*, 112(7), pp. 1947–1952. Available at: http://www.pnas.org/content/112/7/1947.abstract.
Pak, T. (2015) *Saturation tracking and identification of residual oil saturation*. The University of Edinburgh. Available at: https://www.era.lib.ed.ac.uk/handle/1842/17872 (Accessed: 4 May 2017).
Paria, S. (2008) 'Surfactant-enhanced remediation of organic contaminated soil and water', *Advances in Colloid and Interface Science*, pp. 24–58. doi: 10.1016/j.cis.2007.11.001.
Roustaei, A., Saffarzadeh, S. and Mohammadi, M. (2013) 'An evaluation of modified silica nanoparticles' efficiency in enhancing oil recovery of light and intermediate oil reservoirs', *Egyptian Journal of Petroleum*, 22(3), pp. 427–433. doi: 10.1016/j.ejpe.2013.06.010.
Santra, S. *et al.* (2004) 'TAT conjugated, FITC doped silica nanoparticles for bioimaging applications.', *Chemical communications (Cambridge, England)*, (24), pp. 2810–2811. doi: 10.1039/b411916a.
Soga, K., Pagea, J. W. . and Illangasekare, T. . (2004) 'A review of NAPL source

zone remediation efficiency and the mass flux approach', *Journal of Hazardous Materials*, 110(1–3), pp. 13–27. doi: 10.1016/j.jhazmat.2004.02.034.

Tosco, T. *et al.* (2014) 'Nanoscale zerovalent iron particles for groundwater remediation: a review', *Journal of Cleaner Production*, 77, pp. 10–21. doi: 10.1016/j.jclepro.2013.12.026.

Trellu, C. *et al.* (2016) 'Removal of hydrophobic organic pollutants from soil washing/flushing solutions: A critical review', *Journal of Hazardous Materials*, 306, pp. 149–174. doi: 10.1016/j.jhazmat.2015.12.008.

Wang, C. *et al.* (2012) 'Retention and transport of silica nanoparticles in saturated porous media: effect of concentration and particle size.', *Environmental science & technology*, 46(13), pp. 7151–8. doi: 10.1021/es300314n.

Wilson, J. (1990) *Laboratory investigation of residual liquid organics from spills, leaks, and the disposal of hazardous wastes in groundwater*. Edited by R. Kerr. Environmental Research Laboratory, Office of Research and Development, US Environmental Protection Agency, 1990. Available at: https://books.google.co.uk/books?hl=en&lr=&id=wbVNKvmsOxsC&oi=fnd&pg=PR4&dq=Laboratory+investigation+of+residual+liquid+organics+from+spills,+leaks,+and+the+disposal+of+hazardous+wastes+in+groundwater&ots=vrcIBPD7w_&sig=4-29AfAVIZoFxWR9LcZtv3jF7vc (Accessed: 14 July 2017).

Yu, W. and Xie, H. (2012) 'A Review on Nanofluids: Preparation, Stability Mechanisms, and Applications', *Journal of Nanomaterials*. Hindawi Publishing Corp., 2012, pp. 1–17. doi: 10.1155/2012/435873.

Zhang, T. *et al.* (2014) 'Investigation of Nanoparticle Adsorption During Transport in Porous Media', *SPE Journal*, preprint(preprint), pp. 1–11. doi: 10.2118/166346-PA.